Ann. occup. Hyg., Vol. 47, No. 2, pp. 123–144, 2003
Published by Oxford University Press
DOI: 10.1093/annhyg/meg022

Estimating Aerosol Surface Area from Number and Mass Concentration Measurements

ANDREW D. MAYNARD*

National Institute for Occupational Safety and Health, 4676 Columbia Parkway, Cincinnati, OH 45226, USA

Received 11 June 2002; in final form 16 October 2002

A number of toxicology studies have been published indicating that health effects associated with low-solubility inhaled particles may be more appropriately associated with particulate surface area than mass. While exposure data from the workplace is needed to further investigate the relevance of such an association, the means of measuring exposure to aerosol surface area are not readily available. A possible interim solution is to estimate surface area from measurements of particle number and mass concentration using readily available direct-reading instruments. By assuming a lognormal aerosol size distribution with a specific geometric standard deviation, number and mass concentration measurements may be used to estimate the surface area concentration associated with the distribution. Simulations have shown that surface area estimates made on unimodal lognormal aerosols will frequently lie within 100% of the actual value. Simulations using bimodal distributions indicate estimates of surface area vary from the actual value by less than an order of magnitude. Calculations based on experimental unimodal and bimodal data confirm these findings, with estimated surface area rarely being a factor of 4 greater than the actual value, and frequently being much closer than this. These findings indicate that estimating aerosol surface area exposure using readily available number and mass concentration direct-reading instruments may be suitable for providing initial data on the magnitude of surface area exposures with minimal additional effort. This would allow the accumulation of valuable exposure–response data prior to the development and implementation of more sophisticated instrumentation to more accurately estimate surface area exposure.

Keywords: aerosol; surface area; exposure assessment; ultrafine aerosol; number concentration; mass concentration

INTRODUCTION

A number of studies in recent years have demonstrated that response to inhaled low-solubility particles is highly dependent on particle size (Oberdörster *et al.*, 1995; Oberdörster, 2000; Brown *et al.*, 2001). Research has focused on ultrafine particles—typically particles <100 nm in diameter—and has indicated that characterizing exposure to such particles in terms of their mass concentration will lead to their toxicity being severely underestimated. As a result, there has been considerable interest in examining whether characterizing occupational ultrafine aerosol exposure against some metric other than mass is more appropriate. Although research has indicated that particle number concentration may be important, in most cases it appears that both particle number concentration and size play a role in determining response following inhalation. However interpretation of ultrafine particle data in terms of particle surface area leads to a dose response that is independent of particle diameter in many cases (Oberdörster, 2000; Brown *et al.*, 2001). A similar trend has been observed at larger particle diameters (Lison *et al.*, 1997; Driscoll, 1999; Tran *et al.*, 2000), indicating that for low-solubility particles characterizing exposure in terms of surface area will lead to more appropriate exposure limits and evaluation methods.

Validation of this hypothesis requires extensive data relating health effects to aerosol surface area within the workplace. However, aerosol surface area characterization methods are at a relatively early stage of development, and appropriate instrumenta-

*Tel: +1-513-841-4319; fax: +1-513-841-4545; e-mail: zel5@cdc.gov

tion for routine workplace exposure measurements is not generally available. The development and implementation of appropriate aerosol surface area monitors for use in the workplace is dependent on exposure—response data supporting their use. Thus, an impasse exists where the development of instrumentation necessary for exploring how occupational health is associated with aerosol surface area is itself dependent on the very information it will be used to obtain. A possible interim solution that will break the impasse is to consider whether current exposure measurements and methods employed in the workplace can be used to estimate surface area exposure. Real time aerosol mass concentration measurements are routine in many workplaces, and real time number concentration measurements are becoming increasingly routine. It is therefore of considerable interest to consider whether such measurements could be used to estimate aerosol surface area concentration. In this paper the theoretical use of aerosol number and mass concentration measurements to estimate surface area is considered, and errors associated with characterizing a range of aerosol size distributions examined.

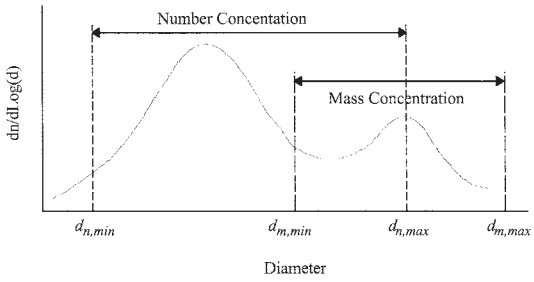

Fig. 1. Schematic representation of the size-dependent detection limits of aerosol number and mass concentration measurements.

BACKGROUND

Although off-line measurements of bulk material surface area have been possible for some time using the BET method (Brunaeur *et al.*, 1938), instruments capable of measuring aerosol surface area in the field are not widely available at present. BET has been used with some success for measuring aerosol surface area. However, it requires the collection of relatively large amounts of material, and measurements are influenced by particle porosity (which may or may not be important) and collection/support substrate—particularly where the quantity of material analyzed is small. The first instrument designed

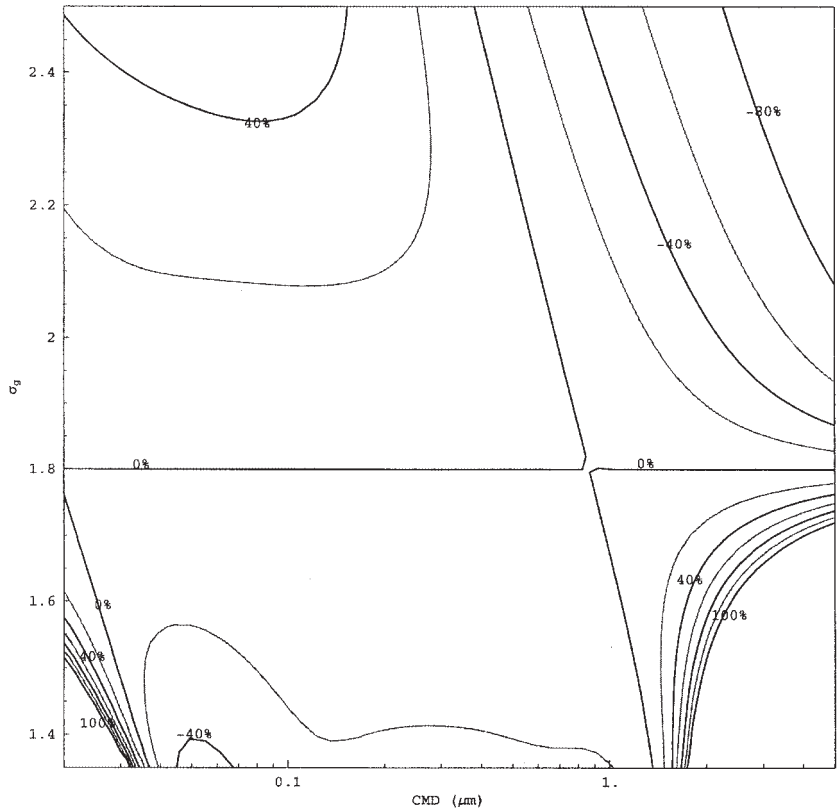

Fig. 2. Plotting %Δ*S* as a function of *CMD* and σ_g for a unimodal lognormal distribution. $\sigma_{g,est}$ = 1.8. Only contours between ±120% are shown.

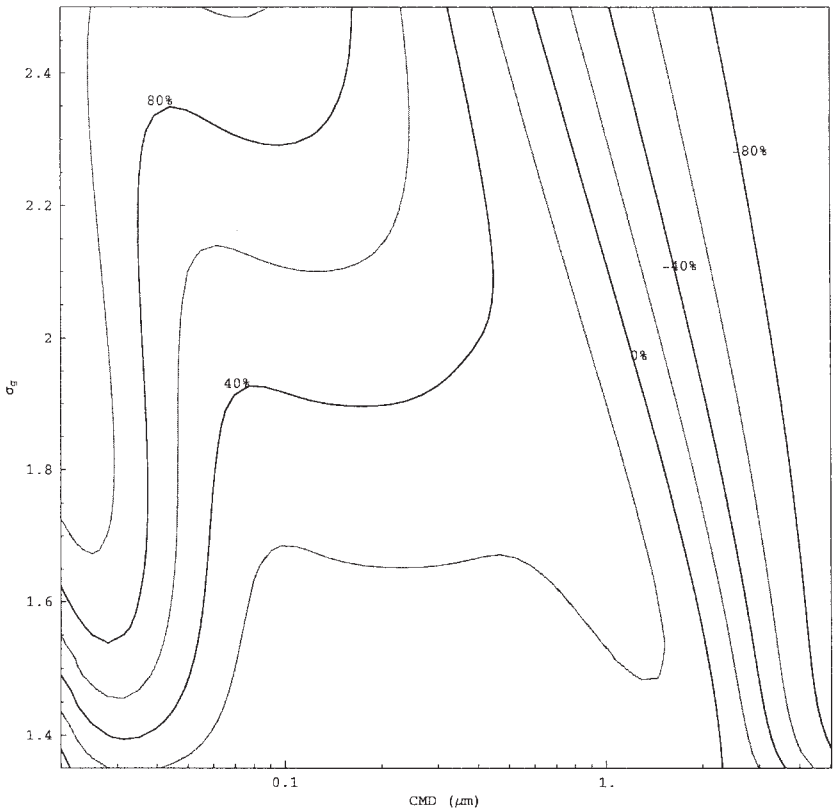

Fig. 3. Plotting %Δ*S* as a function of *CMD* and σ_g for a unimodal lognormal distribution. $\sigma_{g,est}$ = 1.3.

specifically to measure aerosol surface area was the epiphaniometer (Gäggeler *et al.*, 1989; Pandis *et al.*, 1991) (Matter Engineering, Switzerland). This device measures the Fuchs or active surface area of the aerosol by measuring the attachment rate of radioactive ions. As yet it is unknown how relevant active surface area is to health effects following inhalation exposure. Below ~100 nm, active surface scales as the square of particle diameter, and thus is probably a good indicator of actual particle surface area for ultrafine particles. However, above ~1 μm it scales as particle diameter, and so the relationship with actual particle surface area is lost (Gäggeler *et al.*, 1989). The epiphaniometer is not well suited to widespread use in the workplace due to the inclusion of a radioactive source.

The same measurement principle may be applied in the aerosol diffusion charger/electrometer (Keller *et al.*, 2001). The LQ1-DC diffusion charger (Matter Engineering, Switzerland) uses this combination to measure the attachment rate of unipolar ions to particles, and from this the aerosol active surface area is inferred (Baltensperger *et al.*, 2001; Keller *et al.*, 2001). This instrument is also available in a portable form. A similar instrument, the 3070a Aerosol Electrometer, has also recently been developed by TSI Inc. (MN, USA). As in the case of the LQ1-DC the sampled aerosol is charged using a unipolar ion source, and the mean charge measured. However, according to the manufacturer, the 3070a has a response much closer to particle diameter d to the power 1 (d^1).

An alternative method to measuring aerosol surface area is to measure the aerosol size distribution, and to estimate the surface area weighted distribution by assuming a specific particle geometry. Although a number of cascade impactors now have sufficiently small size cut-offs to measure size distributions into the ultrafine aerosol region, the dominant instrument in this area is still the scanning mobility particle sizer (SMPS). The SMPS is capable of measuring aerosol size distribution in terms of mobility diameter from 3 nm up to ~800 nm, although multiple instruments need to be operated in parallel to span this range. The SMPS has the advantage that mobility diameter can be associated with the diameter of a sphere with the same projected area as the particles being sized (Rogak *et al.*, 1993). Thus, transformation of the size distribution to a mean aerosol projected surface area does not require many assumptions about particle shape. The instrument is limited in its widespread application in the workplace however, due to its size, expense, complexity of operation, the need for two or even three instruments

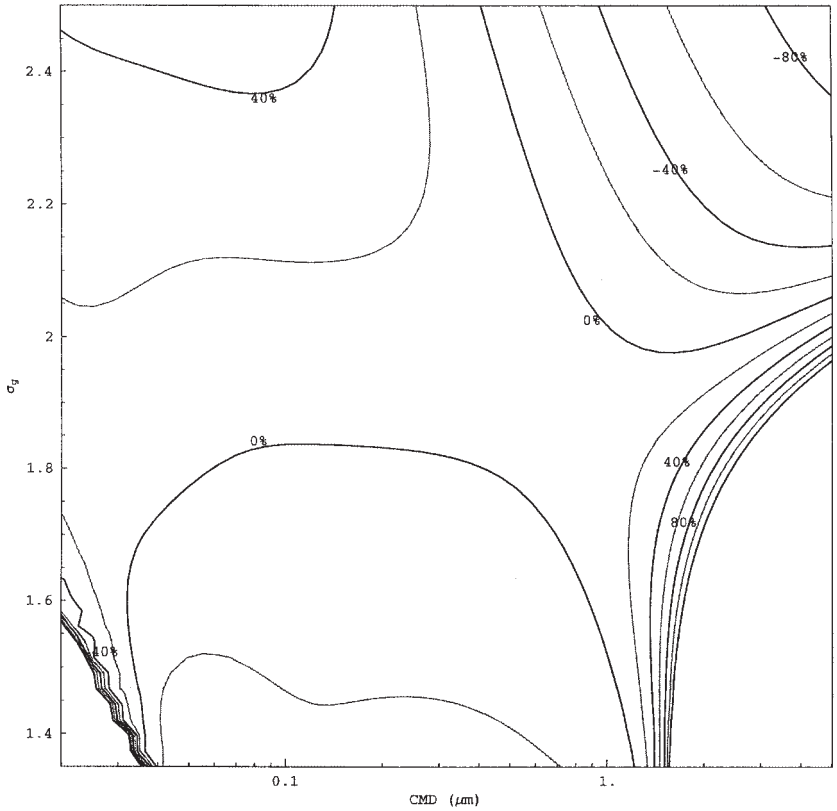

Fig. 4. Plotting mean %Δ*S* as a function of *CMD* and σ_g for a unimodal lognormal aerosol distribution. The mean value of %Δ*S* was estimated using 10 equally spaced values of $\sigma_{g,est}$ ranging from 1.3 to 2.3.

operating in parallel to measure wide aerosol size distributions, and the use of a radioactive source to bring the aerosol to charge equilibrium.

Although each of these instruments has the potential to form the basis of an aerosol surface area measurement method suited for routine use in the workplace, none of them are likely to find widespread application in the near future. Until there is a clear standard for measuring exposure in terms of aerosol surface area, it is unlikely that occupational hygienists or occupational hygiene researchers will invest in unproven, expensive and often complex technology. However, it is also unlikely that the need for measuring exposure against surface area will be demonstrated or disproved without extensive exposure measurements being made in the workplace. One possible option is to wait until current measurement technology has advanced sufficiently for appropriate toxicology and epidemiology studies to be carried out. This would provide a rigorous approach to identifying the most appropriate exposure metric, and developing suitable exposure monitoring methods and exposure limits. Unfortunately, without direct information on health versus exposure to aerosol surface area in the workplace to support such a research effort, this route is likely to be long and tenuous.

An alternative route is to investigate whether current workplace exposure measurements and methods can be used to estimate exposure in terms of aerosol surface area. This has the advantage that currently available methods would be used, thus requiring little or no additional work while collecting exposure data. If measurements could be interpreted to give even a very approximate estimate of surface area, they would open up the possibility of associating health effects with metrics other than mass, and provide supportive evidence for further research into appropriate exposure metrics and evaluation methods. Assuming that the aerosol size distribution is represented well by a unimodal lognormal distribution, it should be possible to estimate the three parameters characterizing it—count median diameter (*CMD*), geometric standard deviation (σ_g) and total concentration—using just three independent measurements. This approach has been proposed by Woo *et al.* (2001) using three simultaneous measurements of aerosol mass concentration, number concentration and charge. Woo *et al.* showed that for ambient aerosols the correlation between estimated and actual surface area was reasonable. However, the reliance on aerosol charge measurements is likely to prevent this technique finding widespread application in the workplace.

The Woo *et al.* method may be modified by assuming one of the distribution parameters, allowing the remaining parameters to be estimated from just two measurements. Aerosol photometers are frequently used to measure aerosol mass concentration in the workplace, and portable condensation particle counters (CPCs) are finding increasing use to measure particle number concentration. Using two such instruments together provides two aerosol measurements on particles between approximately 10 nm and 10 μm, each containing unique information about the size distribution. This is insufficient for estimating the parameters necessary to characterize the aerosol in terms of a unimodal lognormal distribution. Thus, at the outset the use of these two instruments alone to estimate aerosol surface area would seem infeasible. However, if a reasonable estimate could be made of one of the parameters describing the distribution—for instance the geometric standard deviation—the data gathered using the two instruments could be used to estimate the remaining parameters, and give an indication of the aerosol surface area for non-porous particles.

THEORY

If n independent measurements are made on an aerosol, the function $F(x_1, x_2, \ldots, x_m, d)$ that most appropriately describes the size distribution is obtained by minimizing the function

$$\chi^2 = (x_1, x_2, \ldots, x_m, d) = \sum_{i=1}^{n} \left(\frac{C_i - M_i}{\sigma_i} \right)^2 \qquad (1)$$

x_1 to x_m are m parameters describing the size distribution F, d is particle diameter, M_i a measured quantity associated with the aerosol and C_i the expected value of the measurement for an aerosol characterized by distribution F. σ_i is the standard deviation associated with each measurement. C_i is calculated as

$$C_i = \int_{d_{i,\min}}^{d_{i,\max}} F(x_1, x_2, \ldots, x_m, d) R_i(d) \mathrm{d}d \qquad (2)$$

where $R_i(d)$ is the instrument response associated with the measurement M_i. $d_{i,\min}$ and $d_{i,\max}$ represent the size range over which the measurement instrument operates. Where $n \geq m$, equation (1) can be minimized using a range of standard minimization routines and programs. Woo *et al.* (2001) used a subplex routine developed by Rowan (cited in Woo *et al.*) to minimize equation (1) for the case of three independent measurements and an assumed lognormal function.

If a unimodal lognormal particle size distribution is assumed, the distribution function F can be expressed as

$$F(x_1, x_2, \ldots, x_m, d) \equiv N\Phi(CMD, \sigma_g, d) \qquad (3)$$

where $x_1 \equiv N$, $x_2 \equiv CMD$ and $x_3 \equiv \sigma_g$. Φ is the normalized lognormal function. Under this assumption, equation (2) simplifies to

$$C_i = \gamma_i \int_{d_{i,\min}}^{d_{i,\max}} \Phi(\gamma_i MD, \sigma_g, d) \mathrm{d}d \qquad (4)$$

where γ_i represents the total concentration of the quantity being measured, and $\gamma_i MD$ represents the median particle diameter associated with that quantity. γ_iMD is derivable from CMD and σ_g using the Hatch–Choate equations (Hatch and Choate, 1929):

$$\gamma_i MD = CMD e^{b \mathrm{Ln}^2 \sigma_g} \qquad (5)$$

where $b = 3$ when $\gamma_i MD$ is the mass median diameter.

If two independent measurements are made on the same lognormal aerosol, χ^2 will equal zero under the condition

$$\frac{C_1}{C_2} = \frac{M_1}{M_2} \qquad (6)$$

Substituting equation (4) for C_i gives

$$\frac{\gamma_1}{\gamma_2} = \frac{M_1}{M_2} \frac{\int_{d_{2,\min}}^{d_{2,\max}} \Phi(\gamma_2 MD, \sigma_g, d) \mathrm{d}d}{\int_{d_{1,\min}}^{d_{1,\max}} \Phi(\gamma_1 MD, \sigma_g, d) \mathrm{d}d} \qquad (7)$$

If γ_1 represents total aerosol number concentration N, and γ_2 represents total aerosol mass concentration,

$$\gamma_2 = \frac{\pi\rho}{6} d_{\bar{m}}^3 \gamma_1 \qquad (8)$$

assuming spherical particles, where $d_{\bar{m}}$ is the diameter of average mass. $d_{\bar{m}}$ is calculated from the Hatch–Choate equation with $b = 1.5$ (equation 5), giving

$$\frac{\gamma_1}{\gamma_2} = \frac{6}{\pi\rho} \left(CMD e^{1.5 \mathrm{Ln}^2 \sigma_g} \right) \qquad (9)$$

Thus, if σ_g is fixed, equations (7) and (9) can be solved iteratively to yield the ratio γ_1/γ_2 (and consequently CMD and N) from measurements of number and mass concentration. For the case that both M_1 and M_2 are measurements of aerosol number concentration over different size ranges, equations (7) and (9) can be rewritten accordingly to give N as a function of CMD, and solved in a similar manner.

At this point, the aerosol surface area concentration S is given by

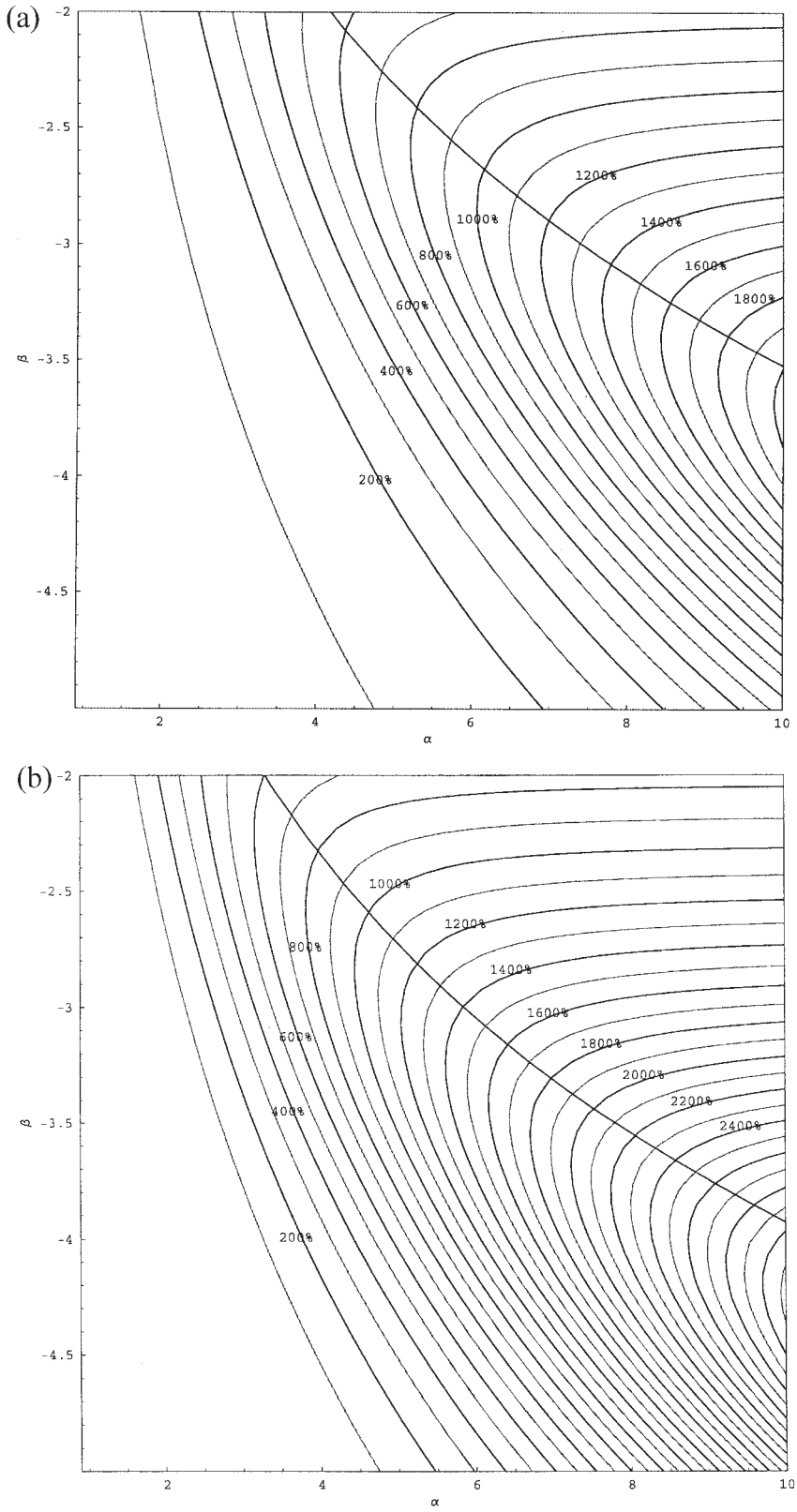
(a)
-2
-2.5
-3
-3.5
-4
-4.5
β
2
4
6
8
10
α
200%
400%
600%
800%
1000%
1200%
1400%
1600%
1800%
(b)
-2
-2.5
-3
-3.5
-4
-4.5
β
2
4
6
8
10
α
200%
400%
600%
800%
1000%
1200%
1400%
1600%
1800%
2000%
2200%
2400%

Fig. 5

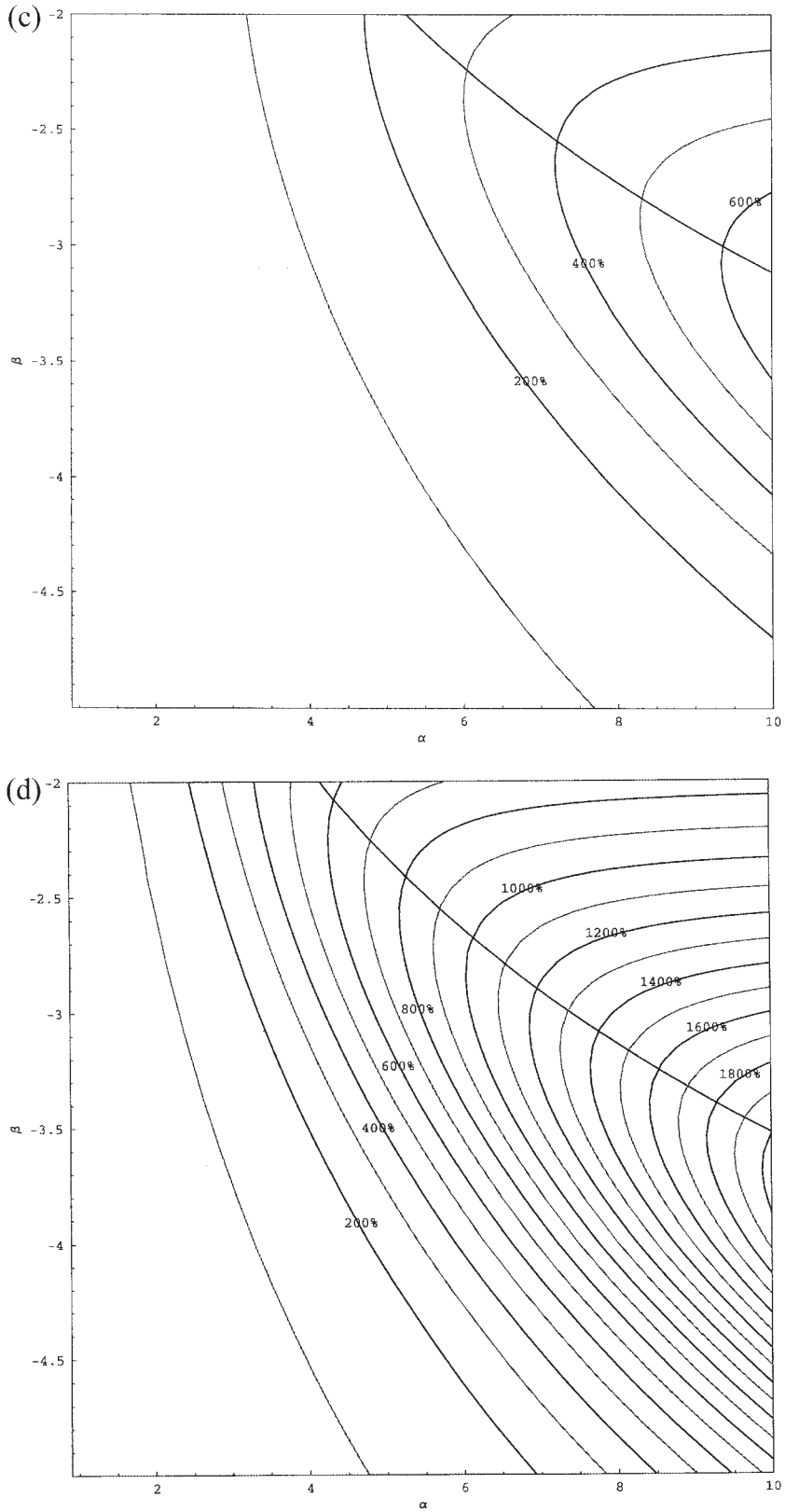

Fig. 5. Plotting %Δ*S* as a function of α and β for a bimodal lognormal aerosol size distribution, assuming infinite sampler detection limits. Each plot is overlaid with the function describing the characteristic ridge feature (equation 17). $\sigma_{g,est}$ = 1.3 and *CMD* = 0.1 μm. (a) $\sigma_{g,1}$ = 1.3, $\sigma_{g,2}$ = 1.3. (b) $\sigma_{g,1}$ = 1.3, $\sigma_{g,2}$ = 2.3. (c) $\sigma_{g,1}$ = 2.3, $\sigma_{g,2}$ = 1.3. (d) $\sigma_{g,1}$ = 2.3, $\sigma_{g,2}$ = 2.3.

$$S = N\pi d_{\bar{s}} \quad (10)$$

where the diameter of average surface area $d_{\bar{s}}$ is given by

$$d_{\bar{s}} = CMDe^{\mathrm{Ln}^2\sigma_g} \quad (11)$$

Solving equations (7) and (9) to find *CMD* and *N* given σ_g is a much more straightforward problem to solve than minimizing equation (1) for three or more variables. If σ_g can be estimated with sufficient accuracy or the method is relatively insensitive to variation in σ_g, and if workplace aerosols of interest can be adequately described by unimodal lognormal size distributions, this approach forms a practical and attractive method for estimating aerosol surface area concentrations from combined number and mass concentration measurements. An example spreadsheet using such calculations to estimate aerosol surface area is given in the Appendix.

ANALYSIS

The accuracy of estimating aerosol surface area concentration using measurements of particle number and mass concentration made with a CPC and a photometer is explored by modeling instrument response to a range of well-characterized aerosol size distributions. For simplicity, the response of each instrument is assumed to be constant for particles having diameters lying within a given response range, and zero outside this range. The lower and upper detection limits for number concentration measurements are defined by $d_{n,\min}$ and $d_{n,\max}$ respectively, and for mass concentration measurements by $d_{m,\min}$ and $d_{m,\max}$ (Fig. 1). In order to provide a set of reference conditions, 'ideal' samplers have been defined as having infinite response ranges. While this is not a physically plausible scenario, it enables the nature of aerosol surface area estimates to be investigated independently of instrument response, and provides a benchmark with which to compare the response of realistic instruments. When modeling estimated surface area using realistic instruments, response ranges are based on those of commercially available devices. The response range of the CPC was set from 20 nm to 1 μm, reflecting that of the TSI P-Trak portable CPC (TSI Inc., MN, USA). The upper limit of 1 μm is somewhat arbitrary as the upper detection limit of a CPC is ill-defined without using a size-selective pre-separator. However in many cases—particularly where ultrafine particle exposure is of concern—total aerosol surface area will be dominated by particles <1 μm. The lower detection limit of the photometer was set to 0.1 μm and the upper limit to 4 μm, corresponding to a respirable size-selective inlet. Although the chosen lower limit is probably lower than the effective lower limit for some aerosols, it was based on the stated lower detection limit of the TSI DustTrak (TSI Inc.). The upper limit of detection for photometers with no size-selective inlet typically lies between 5 and 10 μm. However, it is common for devices to be used with a respirable aerosol pre-separator within the workplace, limiting the upper diameter of detected particles to ~4 μm.

The particle number and mass concentrations that would be measured for a given aerosol distribution is calculated by integrating the number or mass weighted distribution between the instrument detection limits. Two categories of aerosol distribution are considered: unimodal lognormal distributions and bimodal lognormal distributions. In the case of modeling instrument response to unimodal lognormal distributions equation (4) is used to calculate the measured aerosol concentration. Similarly for bimodal distributions equation 4 is used to model the measured aerosol concentration associated with each mode, and the values summed to give the total modeled measured concentration value. It is assumed in all cases that measurement errors are negligible.

In each case, modeled concentration measurements are used to estimate aerosol surface area concentration by numerically solving equations (6) and (8) with an assumed value of σ_g ($\sigma_{g,est}$) to derive estimated values of *CMD* and *N*. The difference between estimated and actual surface area is expressed as either S_R or $\%\Delta S$:

$$S_R = \frac{S_{\mathrm{est}}}{S_{\mathrm{actual}}}$$

$$\%\Delta S = 100\frac{S_{\mathrm{est}} - S_{\mathrm{actual}}}{S_{\mathrm{actual}}} \quad (12)$$

where S_{est} is the estimated surface area concentration and S_{actual} the actual surface area concentration. S_R provides a measure of the relative difference between S_{est} and S_{actual}, and is useful for when the difference between the two quantities is large, and in particular where S_{est} is smaller than S_{actual}. $\%\Delta S$ gives a more intuitive understanding of the comparison between S_{est} and S_{actual} where the differences are not too large, and provides an indication of the error associated with the estimated value. In most cases $\%\Delta S$ is used in preference to S_R for assessing the differences between the estimated and actual values of aerosol surface area.

UNIMODAL LOGNORMAL DISTRIBUTIONS

Given the construct of the model, when the estimated or assumed aerosol geometric standard deviation is equivalent to σ_g for a unimodal distribution, $\%\Delta S$ is always zero. Applying the method to unimodal lognormal distributions was therefore

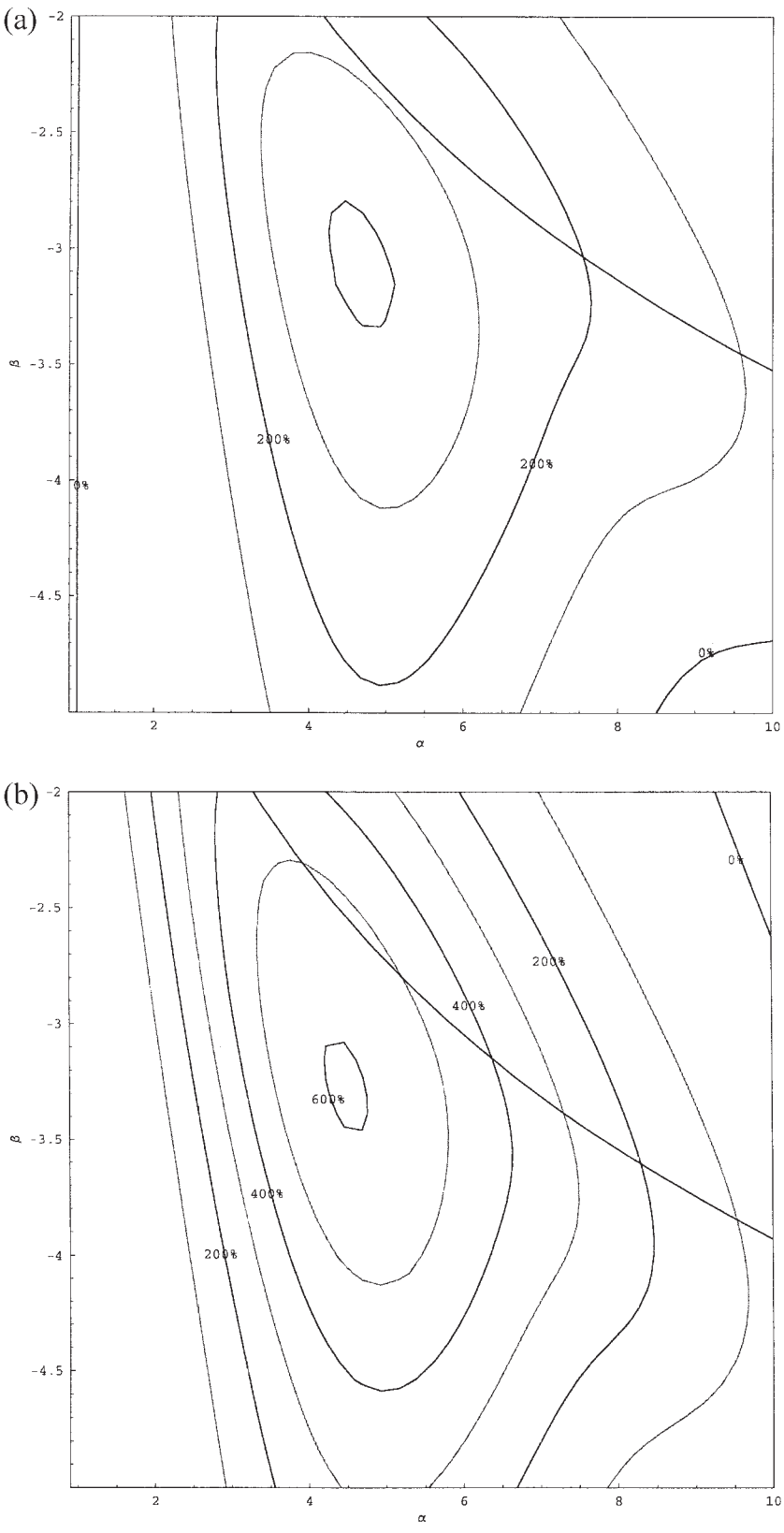
(a)
-2
-2.5
-3
-3.5
-4
-4.5
β
200%
200%
0%
0%
2
4
6
8
10
α
(b)
-2
-2.5
-3
-3.5
-4
-4.5
β
0%
200%
400%
600%
400%
200%
2
4
6
8
10
α

Fig. 6

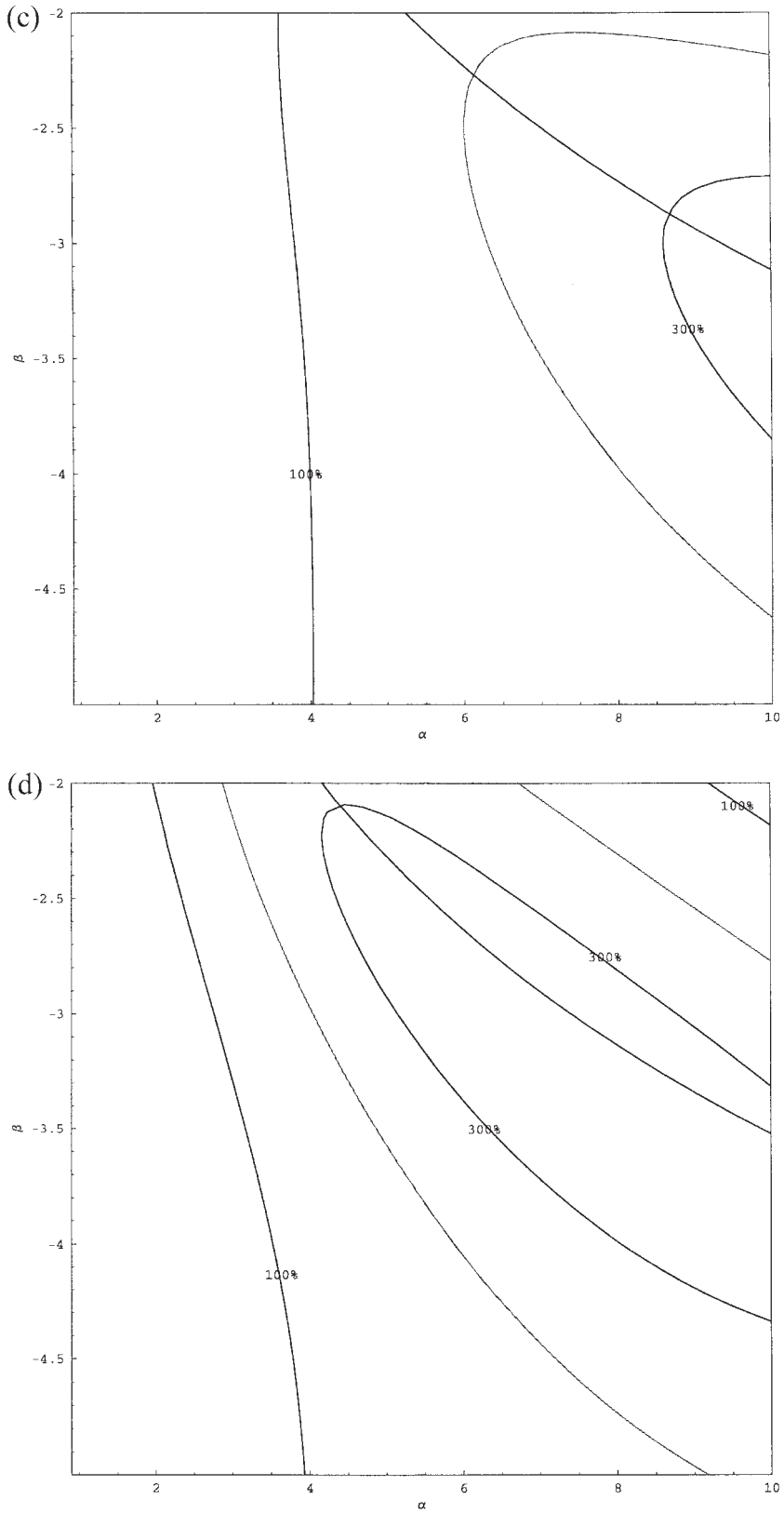

Fig. 6. Plotting %Δ*S* as a function of α and β for a bimodal lognormal aerosol size distribution, assuming realistic sampler detection limits. $\sigma_{g,est}$ = 1.3 and *CMD* = 0.1 μm. Each plot is overlaid with the function describing the characteristic ridge feature (equation 17). (a) $\sigma_{g,1}$ = 1.3, $\sigma_{g,2}$ = 1.3. (b) $\sigma_{g,1}$ = 1.3, $\sigma_{g,2}$ = 2.3. (c) $\sigma_{g,1}$ = 2.3, $\sigma_{g,2}$ = 1.3. (d) $\sigma_{g,1}$ = 2.3, ι = 2.3.

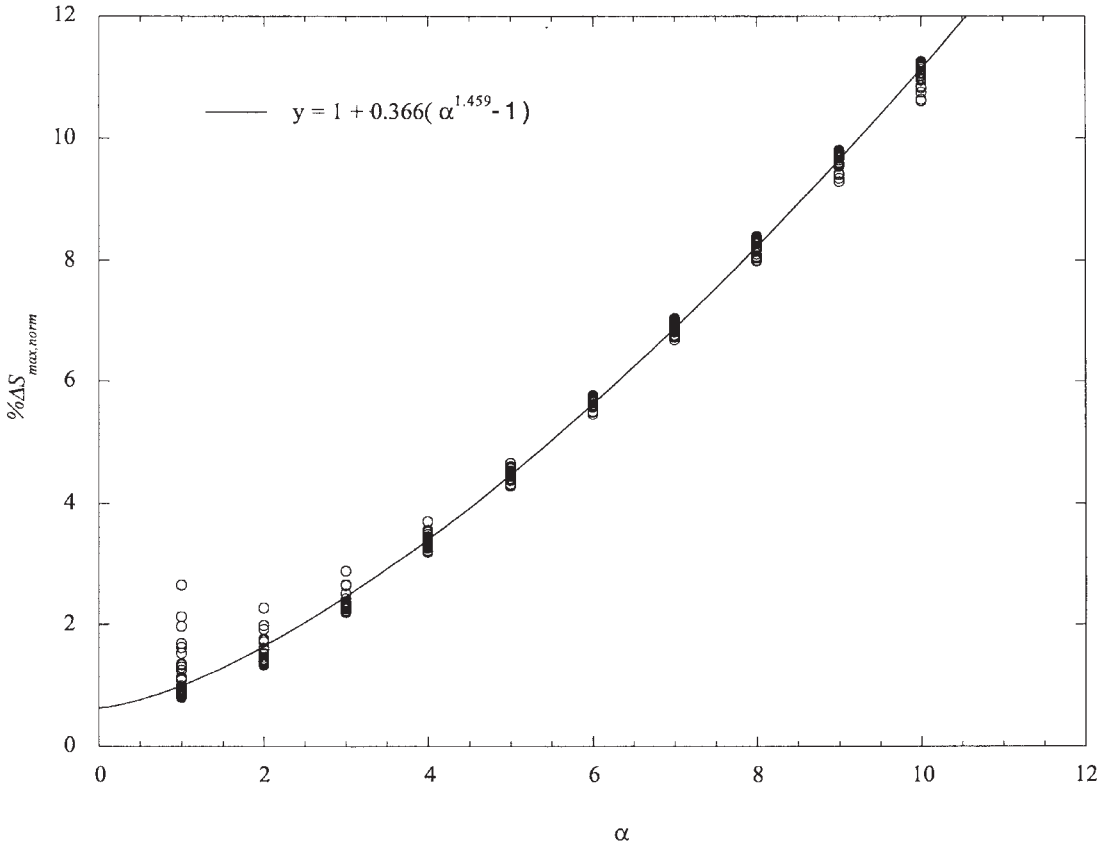

Fig. 7. Plotting $\%\Delta S_{max,norm}$ versus α for $1.3 < \sigma_{g,1} < 2.3$, $1.3 < \sigma_{g,2} < 2.3$ and $1.3 < \sigma_{g,est} < 2.3$.

investigated by evaluating $\%\Delta S$ for $\sigma_{g,est} \neq \sigma_g$ over a range of *CMD*. $\sigma_{g,est}$ was nominally set to 1.8, based on size distribution data from Zimmer and Maynard (2002). Calculating $\%\Delta S$ as a function of *CMD* and σ_g, assuming ideal samplers showed that estimated error is independent of *CMD*, and only depended on the difference between σ_g and $\sigma_{g,est}$. Within the range $1.3 < \sigma_g < 2.5$, estimated error was typically within the range –20% to 60%.

Figure 2 presents the results of the same calculations as a contour plot of $\%\Delta S$ versus *CMD* and σ_g, but assuming realistic instrument detection limits, as given above. With the introduction of finite instrument detection limits, a dependency between $\%\Delta S$ and *CMD* was introduced. This is most apparent for small σ_g at the upper and lower limits of the *CMD* values used, where estimated error increases rapidly. However, at larger σ_g, and in the region defined by $d_{n,\min} < CMD < d_{m,\max}$, the estimated error is constrained between relatively narrow bounds. Although the relative plots are not shown, decreasing $d_{n,\min}$ and increasing $d_{m,\max}$ had a tendency to reduce the estimated error associated with low and high values of *CMD*, and led to plots that tend to the case for ideal samplers.

The effect of the choice of $\sigma_{g,est}$ on $\%\Delta S$ can be qualitatively understood from Fig. 2. The plot is divided into regions defined by $\sigma_g = \sigma_{g,est}$, with $\%\Delta S = 0\%$ at $\sigma_g = \sigma_{g,est}$. Varying $\sigma_{g,est}$ will move this dividing line up or down accordingly, resulting in a better or poorer estimate of the aerosol surface area, depending on the actual distribution's σ_g and *CMD*. Figure 2 indicates that lower values of $\sigma_{g,est}$ may be beneficial in reducing the maximum values of $\%\Delta S$ likely to be experienced. The results for $\sigma_{g,est} = 1.3$ are plotted in Fig. 3. Within the bounds of σ_g and *CMD* chosen, estimated error is now bound between ±90% ($0.1 < S_R < 1.9$).

The effect of assuming a range of $\sigma_{g,est}$ and averaging the resulting values of S_{est} was also investigated over a range of σ_g and *CMD*. Figure 4 shows the contour plot of $\%\Delta S$ versus *CMD* and σ_g with contours representing equal values of mean $\%\Delta S$, calculated using 10 values of $\sigma_{g,est}$ between 1.3 and 2.3. As the mean value of $\sigma_{g,est}$ was 1.8, Fig. 4 is directly comparable with Fig. 2. Evaluating mean $\%\Delta S$ over a range of $\sigma_{g,est}$ had the effect of marginally increasing the plot area for which $\%\Delta S$ lies between ±20%. However, there was little change in the estimated error at low and high values of *CMD*.

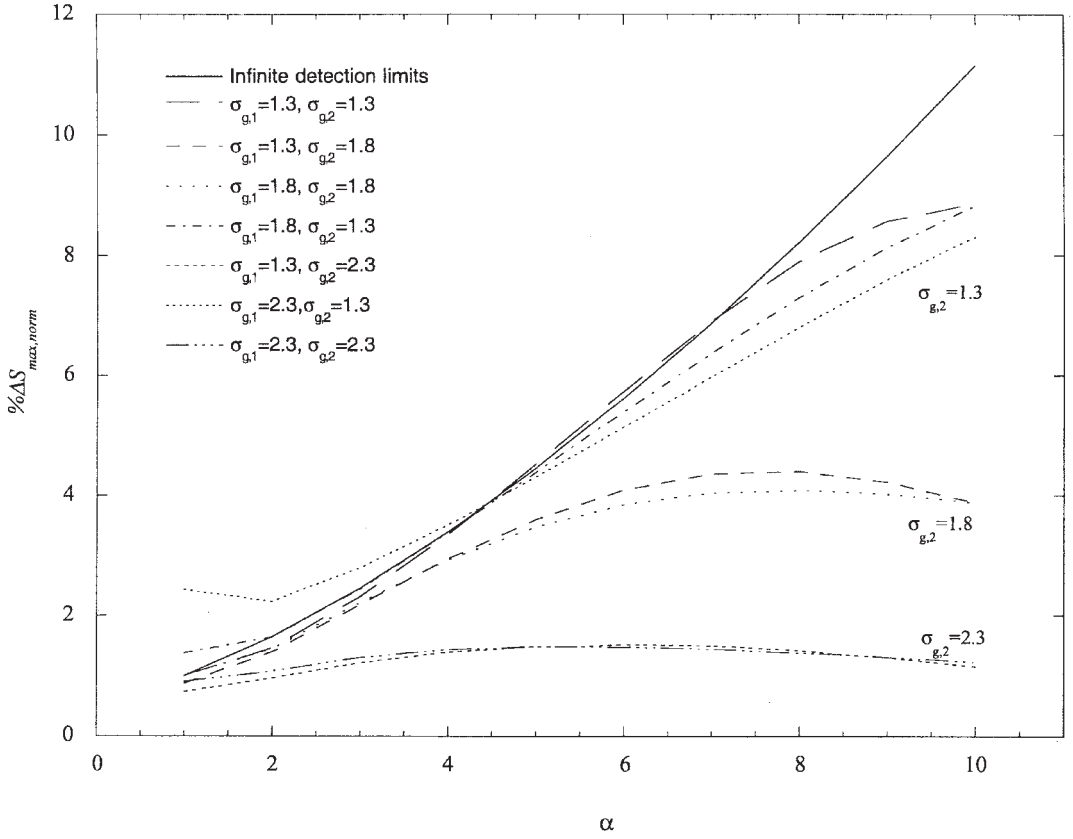

Fig. 8. Plotting $\%\Delta S_{max,norm}$ versus α for a range of $\sigma_{g,1}$ and $\sigma_{g,2}$. *CMD* = 0.1 μm, $\sigma_{g,est}$ = 1.3. Where finite detection limits are assumed, $d_{n,min}$ = 0.02 μm, $d_{n,max}$ = 1 μm, $d_{m,min}$ = 0.1 μm and $d_{m,max}$ = 4 μm.

BIMODAL LOGNORMAL DISTRIBUTIONS

Using aerosol number and mass concentrations to estimate surface area assumes a unimodal lognormal distribution. This assumption is most poorly representative of bimodal distributions (assuming that the addition of further modes between the two initial modes can only act to bring the overall distribution closer to the assumed unimodal distribution). Bimodal distributions also represent the extremes of workplace aerosols where both nucleation and mechanical generation processes take place. Thus, modeling the error associated with estimating the surface area of a bimodal distribution from number and mass concentration measurements allows the limitations of the method to be explored in detail.

An analytical understanding of how estimated surface area is influenced by the aerosol distribution and the instrument operating parameters is highly complex given the non-linear relationship between some significant factors. A simplified analysis is therefore presented that enables the development of a semi-quantitative understanding of how various parameters are likely to affect estimates of aerosol surface area. Each aerosol size distribution is defined as the sum of two lognormal distributions, where CMD_1, $\sigma_{g,1}$ and N_1 define the mode with the smaller modal diameter, and CMD_2, $\sigma_{g,2}$ and N_2 define the mode with the larger modal diameter. The relationship between the aerosol number concentration associated with each mode is characterized by the exponent β

$$\frac{N_2}{N_1} = 10^{\beta} \tag{13}$$

Likewise, the relationship between the *CMD* of the lower and upper modes is characterized by the factor α

$$\frac{CMD_1}{CMD_2} = \frac{1}{\alpha^2} \tag{14}$$

giving

$$CMD_1 = \frac{\overline{CMD}}{\alpha}, CMD_2 = \alpha\overline{CMD} \tag{15}$$

where $\overline{CMD}$ is the geometric mean of CMD_1 and CMD_2. Thus, as β increases the number of particles

associated with the larger diameter mode increases rapidly. Likewise, as α increases, the difference in median diameter between the modes increases.

Figure 5 plots contours of equal $\%\Delta S$ as a function of α and β for a range of $\sigma_{g,1}$ and $\sigma_{g,2}$, in each case assuming $\sigma_{g,est} = 1.3$ and infinite sampler detection limits. Evaluating the plots with different values of $\sigma_{g,est}$ affected only the values of the contours, and not the form of the plots (for a given α and β, $\%\Delta S$ decreases as $\sigma_{g,est}$ increases). As the sampler detection limits were assumed to be infinite, carrying out the evaluation with different values of $\overline{CMD}$ had no effect on the results. Each plot has a characteristic feature, or ridge, defining a sharp change in direction of the contour lines. The function describing this ridge may be estimated by assuming points defining the feature occur when the surface area associated with the upper mode is equal to that associated with the lower mode, weighted by some factor w. A weighting factor of

$$w = 3\frac{e^{0.5\mathrm{Ln}^2\sigma_{g,2}}}{e^{0.5\mathrm{Ln}^2\sigma_{g,1}}} \quad (16)$$

was empirically found to allow the set of α and β to be estimated that define the ridge, giving

$$\beta_{\mathrm{ridge}} = \mathrm{Ln}\left(\frac{3}{\alpha^4}\frac{e^{1.5\mathrm{Ln}^2\sigma_{g,1}}}{e^{1.5\mathrm{Ln}^2\sigma_{g,2}}}\right) \quad (17)$$

Although equation (17) does not match the ridge feature exactly in Fig. 5, it is sufficiently close to represent a characteristic feature of these plots. More significantly, it provides an analytical function describing pairs of α and β that give an approximation of the maximum errors associated with a range of bimodal lognormal distributions, assuming infinite aerosol detection limits. Evaluating $\%\Delta S$ as a function of α and β while assuming realistic instrument detection limits resulted in markedly different plots. Figure 6 shows the results of the same analysis as for Fig. 5, but with instrument detection limits of $d_{n,\min} = 0.02$ μm, $d_{n,\max} = 1$ μm, $d_{m,\min} = 0.1$ μm and $d_{m,\max} = 4$ μm. In each case $\%\Delta S$ for a given α and β is reduced. For both plots where $\sigma_{g,1} = 2.3$ (Fig. 6c,d) equation (17) represents the ridge feature well. For $\sigma_{g,1} = 1.3$ (Fig. 6a,b) the form of the plot varies markedly, with a second ridge feature becoming apparent. However, equation (16) still gives a reasonable representation of the main ridge representing high values of $\%\Delta S$. Thus, within reasonable limits, the data points defined by equation (17) can be taken to estimate a ridge of high $\%\Delta S$ for finite instrument detection limits. Evaluating how $\%\Delta S$ varies along this line therefore provides a means of estimating the effect of changes in a number of parameters on $\%\Delta S$. For clarity, values of $\%\Delta S$ along the line defined by equation (17) are denoted by $\%\Delta S_{\max}$.

If infinite detection limits are assumed, $\%\Delta S_{\max}$ is a function of $\sigma_{g,1}$, $\sigma_{g,2}$, $\sigma_{g,est}$ and α. The dependency of $\%\Delta S_{\max}$ on $\sigma_{g,1}$, $\sigma_{g,2}$ and $\sigma_{g,est}$ can be approximated by

$$\%\Delta S_{\max} = F(\alpha) \times 100\frac{e^{\mathrm{Ln}^2\sigma_{g,2}}}{e^{\mathrm{Ln}^2\sigma_{g,1}}}\frac{e^{\mathrm{Ln}^2\sqrt{\sigma_{g,1}\sigma_{g,2}}}}{e^{\mathrm{Ln}^2\sigma_{g,est}}} - 100 \quad (18)$$

where $F(\alpha)$ is some function of α. Plotting normalized $\%\Delta S_{\max}$ against α allows a suitable empirical form of the function $F(\alpha)$ to be derived, where normalized $\%\Delta S_{\max}$ is defined as

$$\%\Delta S_{\max,\mathrm{norm}} = (\%\Delta S_{\max} + 100) \quad (19)$$

$$\times \frac{1}{100}\frac{e^{\mathrm{Ln}^2\sigma_{g,1}}}{e^{\mathrm{Ln}^2\sigma_{g,2}}}\frac{e^{\mathrm{Ln}^2\sigma_{g,est}}}{e^{\mathrm{Ln}^2\sqrt{\sigma_{g,1}\sigma_{g,2}}}} = F(\alpha)$$

(Fig. 7). $F(\alpha)$ may be approximated by

$$F(\alpha) = 1 + a(\alpha^b - 1) \quad (20)$$

ensuring that equation (18) reduces to $\%\Delta S_{\max} = 0$ for a unimodal distribution with $\sigma_{g,est} = \sigma_g$. Applying a least-square fit to the data in Fig. 7 leads to $a = 0.366$ and $b = 1.459$. Equation (18) implies that $\%\Delta S_{\max}$ is more strongly influenced by $\sigma_{g,2}$ than either $\sigma_{g,1}$ or $\sigma_{g,est}$.

Introducing finite instrument detection limits clearly has a significant effect on $\%\Delta S_{\max}$, as is shown in the comparison between Figs 5 and 6. The effect of changes in these detection limits on the maximum error associated with surface area estimates for bimodal distributions may be qualitatively evaluated by evaluating $\%\Delta S_{\max}$ under different conditions. It is clear that any dependency between $\%\Delta S_{\max}$ and CMD with finite detection limits is only dependent on the ratio between the detection limits and CMD. Thus, defining normalized detection limits as

$$d(\mathrm{norm})_{n,\min} = \frac{d_{n,\min}}{\overline{CMD}} \quad (21)$$

$$d(\mathrm{norm})_{n,\max} = \frac{d_{n,\max}}{\overline{CMD}}$$

$$d(\mathrm{norm})_{m,\min} = \frac{d_{m,\min}}{\overline{CMD}}$$

$$d(\mathrm{norm})_{m,\min} = \frac{d_{m,\min}}{\overline{CMD}}$$

allows the dependency on $\overline{CMD}$ to be removed. Plotting $\%\Delta S_{\max,\mathrm{norm}}$ with finite detection limits for a range of $\sigma_{g,1}$ and $\sigma_{g,2}$ clearly shows that for a fixed

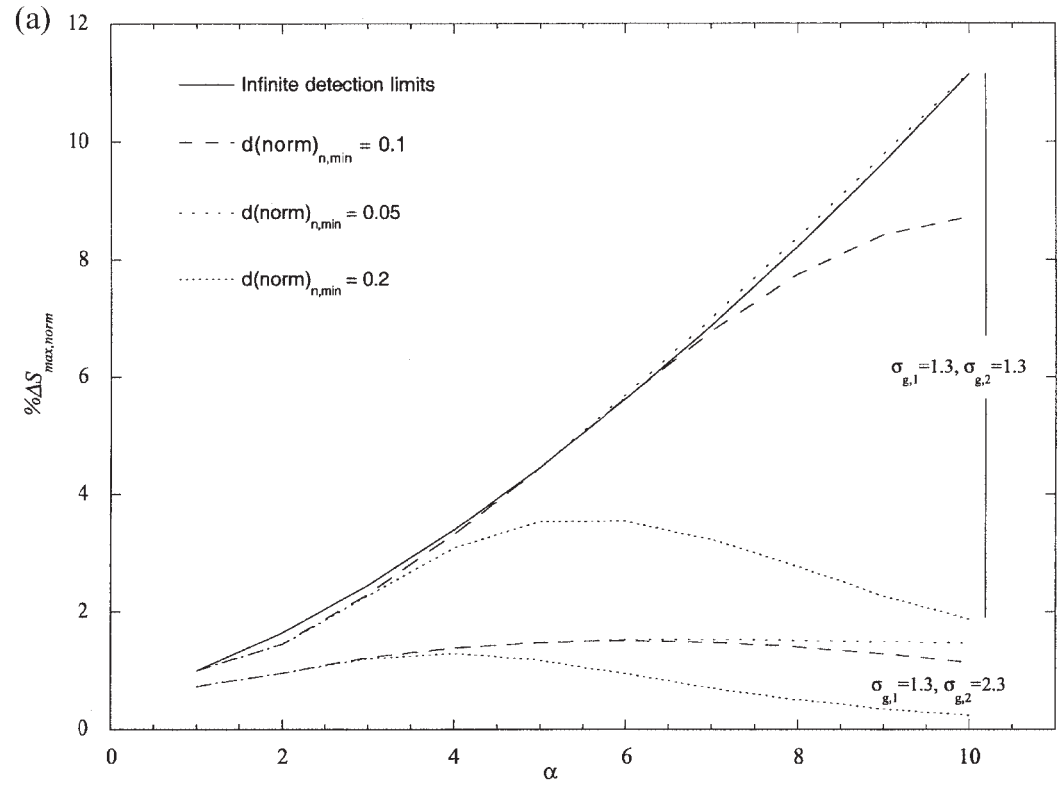
(a)
Infinite detection limits
d(norm)n,min = 0.1
d(norm)n,min = 0.05
d(norm)n,min = 0.2
σg,1=1.3, σg,2=1.3
σg,1=1.3, σg,2=2.3
%ΔSmax,norm
α

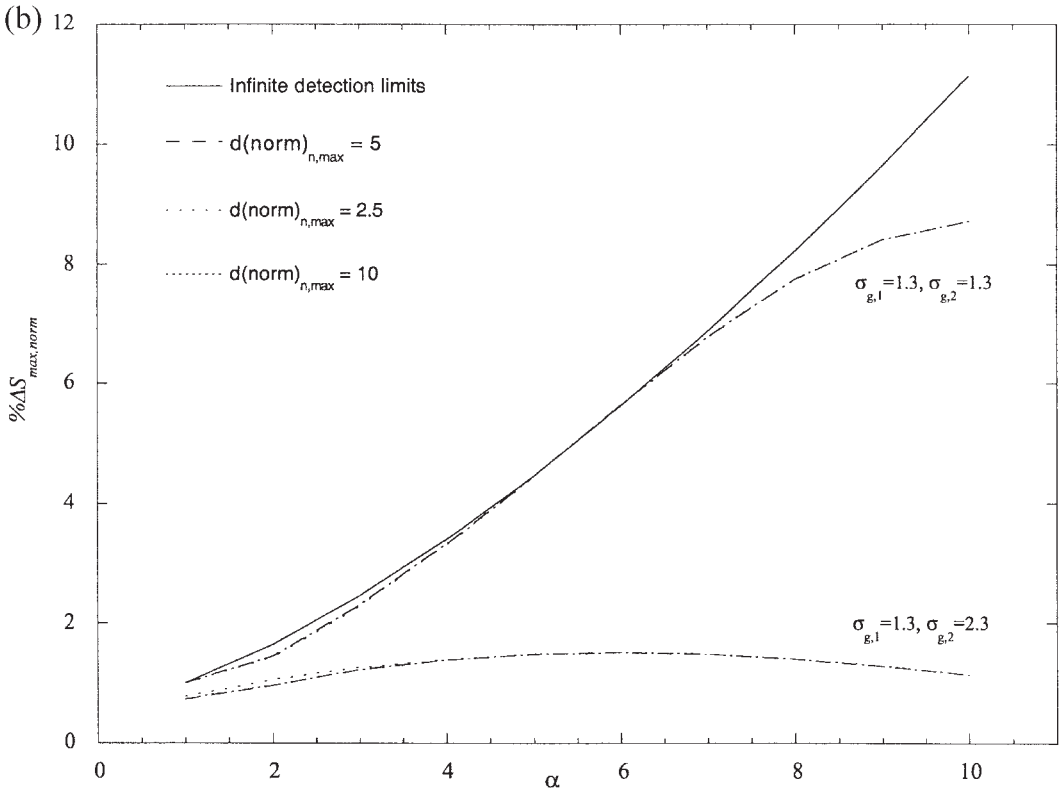
(b)
Infinite detection limits
d(norm)n,max = 5
d(norm)n,max = 2.5
d(norm)n,max = 10
σg,1=1.3, σg,2=1.3
σg,1=1.3, σg,2=2.3
%ΔSmax,norm
α

Fig. 9

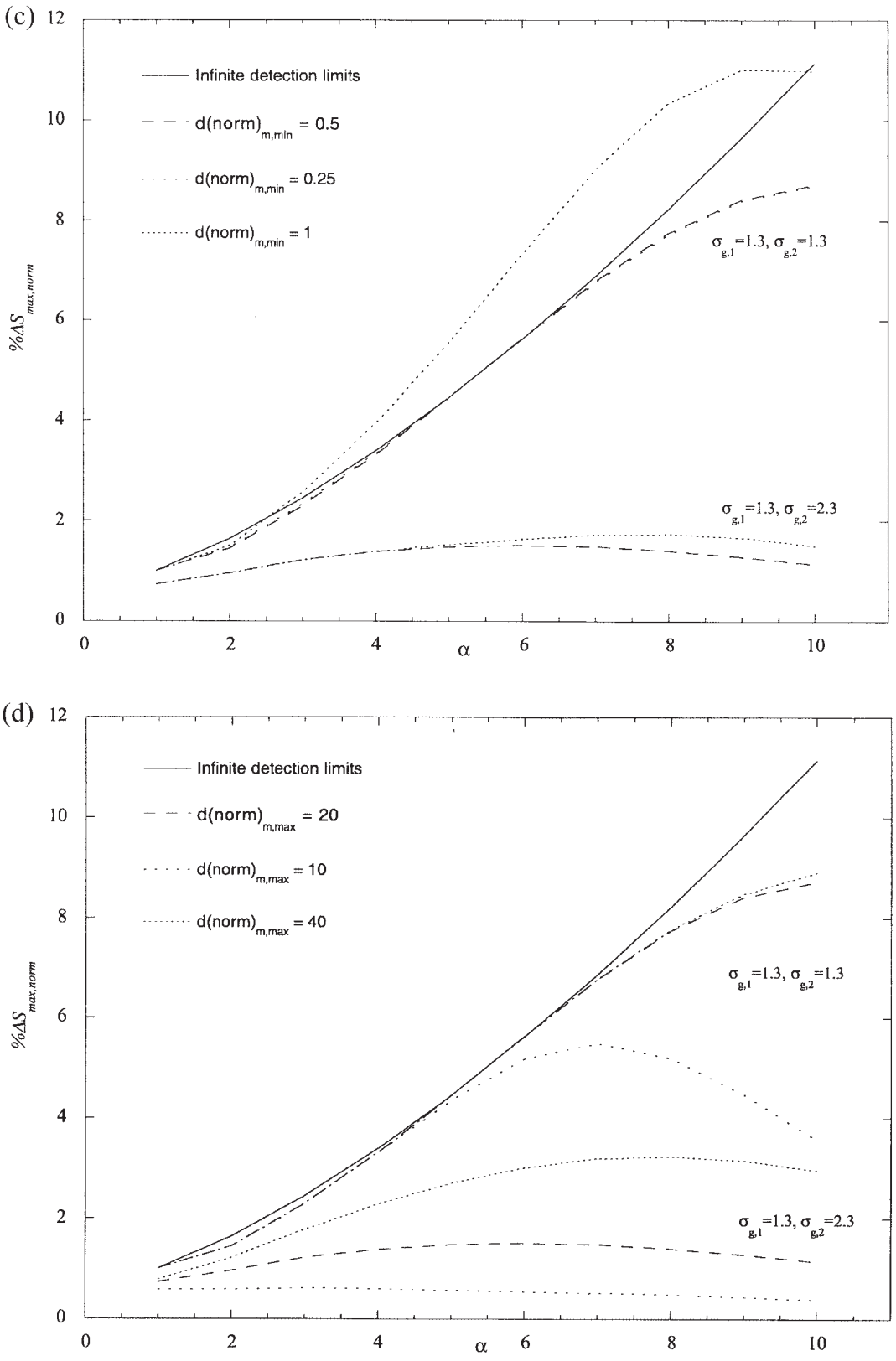

Fig. 9. Plotting $\%\Delta S_{max,norm}$ versus α while independently varying normalized detection limits. In each case $\sigma_{g,est} = 1.3$. Baseline detection limits are $d(\text{norm})_{n,\min} = 0.1$, $d(\text{norm})_{n,\max} = 5$, $d(\text{norm})_{m,\min} = 0.5$ and $d(\text{norm})_{m,\max} = 20$. (a) $0.05 < d(\text{norm})_{n,\min} < 0.2$. (b) $2.5 < d(\text{norm})_{n,\max} < 10$. (c) $0.25 < d(\text{norm})_{m,\min} < 1$. (d). $10 < d(\text{norm})_{m,\max} < 40$.

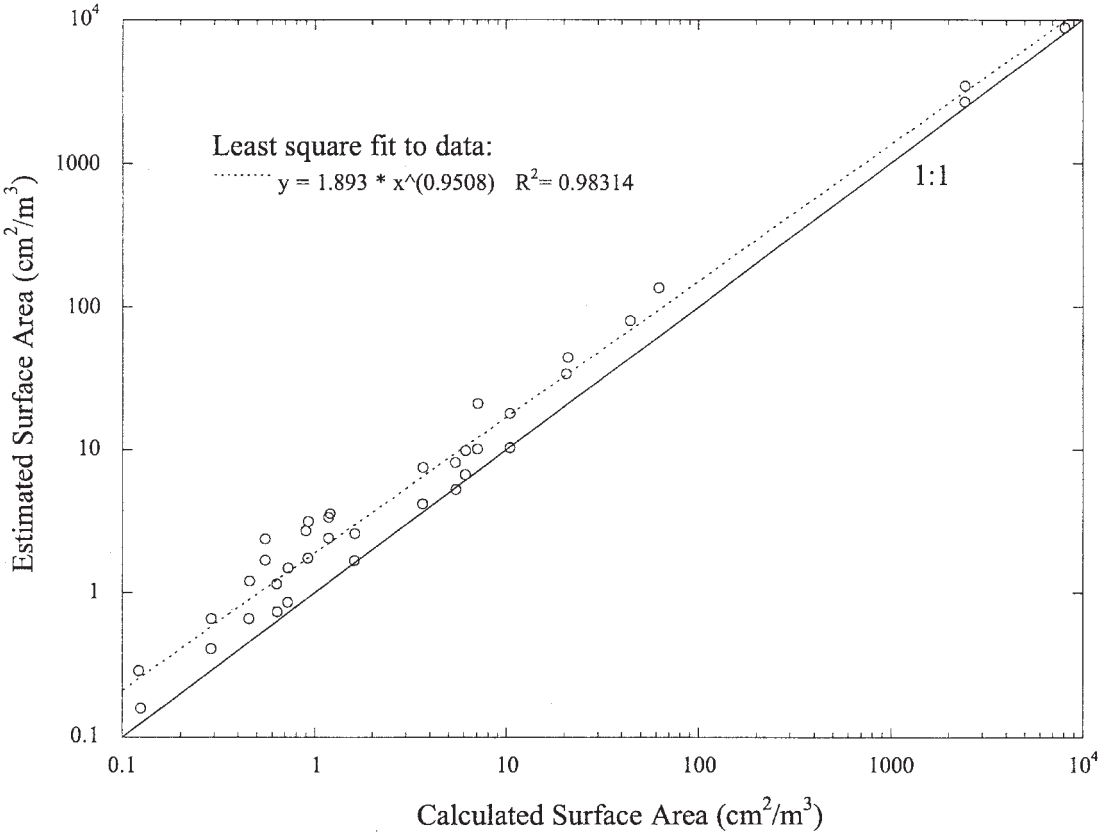

Fig. 10. Plotting estimated surface area versus calculated surface area from distributions in McCawley *et al.* (2001) and Zimmer and Maynard (2002), assuming $\sigma_{g,est} = 1.3$ and 1.8 (Tables 1 and 2). Applying a least-square fit to surface area estimates using $\sigma_{g,est} = 1.8$ alone gives $y = 1.51x^{0.96}$, $R^2 = 0.99988$.

$\overline{CMD}$ and $\sigma_{g,est}$, $\sigma_{g,2}$ is the dominant factor in determining the accuracy of surface area estimates (Fig. 8). Evaluating $\%\Delta S_{max}$ between realistic limits of $\sigma_{g,2}$ therefore enables the envelope of typical maximum errors to be visualized over a range of conditions—in this investigation the range $1.3 < \sigma_{g,2} < 2.3$ is used.

The effect of varying each instrument detection limit independently of the others is demonstrated in Fig. 9. In each case, the selected detection limit is increased or decreased by a factor of 2 about a geometric midpoint diameter. Baseline detection limits of $d(\text{norm})_{n,\text{min}} = 0.1$, $d(\text{norm})_{n,\text{max}} = 5$, $d(\text{norm})_{m,\text{min}} = 0.5$ and $d(\text{norm})_{m,\text{max}} = 20$ are used, corresponding to previously stated typical detection limits for $\overline{CMD} = 0.2$ μm. The most marked deviations in response are associated with varying $d(\text{norm})_{n,\text{min}}$ and $d(\text{norm})_{m,\text{max}}$. In each of these cases, reducing the range of aerosol particles detected decreases the maximum detection error. Increasing $d(\text{norm})_{m,\text{min}}$ above 0.5 leads to a rapid increase in maximum error. This detection limit typically lies between the two modes of the modeled aerosol distributions, and it appears that above a certain point estimates of aerosol surface area may become particularly sensitive to changes in its value. Within the limits of the analysis, maximum estimated error is relatively insensitive to changes in $d(\text{norm})_{n,\text{max}}$.

EXPERIMENTALLY MEASURED AEROSOL SIZE DISTRIBUTIONS

Experimentally measured aerosol size distributions from two investigations have been used to compare actual aerosol surface area with that which would be estimated from measurements of number and mass concentration. These studies are unique in that they present size data down to nanometer diameters, and thus allow the method to be evaluated into the ultrafine aerosol region. McCawley *et al.* (2001) have published data on aerosol size distributions in the sub-micrometer region arising from various processes involving beryllium processing. Number concentration data are truncated at 0.37 μm, preventing an estimation of the aerosol surface area that may have been associated with larger particles. However, the data provide a good representation of unimodal distributions dominated by thermal generation processes. The second dataset comes from high speed grinding on a number of substrates (see Table 2) (Zimmer and Maynard, 2002), and represents particle size distribu-

Table 1. S_R calculated using measured aerosol size distributions from McCawley *et al.* (2001), assuming $\sigma_{g,est}$ = 1.3, and $\sigma_{g,est}$ = 1.8. $d_{n,min}$= 0.02 μm, $d_{n,max}$ = 1 μm, $d_{m,min}$ = 0.1 μm, $d_{m,max}$ = 4 μm

Process area	Lognormal fit to data		$\sigma_{g,est}$ = 1.3		$\sigma_{g,est}$ = 1.8	
	CMD (nm)	σ_g	Estimated surface area (cm^2/m^3)	S_R	Estimated surface area (cm^2/m^3)	S_R
Arc furnace	49.18	1.68	2.59	1.60	1.68	1.04
Reduction furnace	40.69	1.79	18.01	1.72	10.35	0.99
Solution preparation	43.50	1.91	9.83	1.60	6.73	1.10
Rod bar and tube	51.36	1.84	8.14	1.50	5.29	0.97
Old cast shop (1)	18.79	1.96	7.53	2.05	4.21	1.15
Impact grinder	26.53	1.64	0.29	2.38	0.16	1.28
Fluoride furnace (1)	No fit	11358.00	1.40	8804.4	1.09	
4 hi furnace	37.70	1.49	1.49	2.05	0.86	1.19
Oxides	No fit	3438.60	1.41	2665.7	1.10	
Old cast shop (2)	31.11	1.33	1.21	2.64	0.66	1.45
Be machining (bimodal distribution)	14.43	1.83	0.66	2.27	0.41	1.42
	140.11	1.07				
New cast shop	38.71	1.71	1.15	1.82	0.74	1.16
Fluoride furnace (2)	25.56	1.40	21.08	2.98	10.14	1.44

tions arising from thermal and mechanical processes simultaneously between 5 nm and 20 μm. In many cases the distributions are bimodal with the lower mode (CMD_1) around 10 nm and the upper mode (CMD_2) above 1 μm. In many situations involving thermal aerosol generation the modal diameter will be significantly higher than 10 nm due to rapid particle agglomeration taking place. Thus, the data from Zimmer and Maynard perhaps represent some of the worst scenarios likely to be encountered in the workplace.

The actual surface area for each distribution was calculated by numerically integrating the distribution over the measured size range, assuming spherical particles. Estimates of particle number and mass concentration that would have been measured using a CPC or photometer were made by numerically integrating the distributions over the instrument detection limits. Surface area was then estimated from these values using equations (7) and (9) with estimated geometric standard deviation ($\sigma_{g,est}$) values of 1.3 and 1.8, and the results reported as estimated surface area and S_R.

Table 1 presents the data from McCawley *et al.*, including the *CMD* and σ_g characterizing the least square lognormal fit to each dataset. Using a value of $\sigma_{g,est}$ of 1.3 leads to the estimated surface area lying between 0.5 and 3 times the actual value. Assuming $\sigma_{g,est}$ = 1.8 reduces this range considerably to between 0.95 and 1.45 times the actual value. In each case, the two datasets representing the highest aerosol surface area (fluoride furnace and old cast shop) have values of S_R that are reasonably close to 1. σ_g values from the lognormal fits lie closer to 1.8 than 1.3 in most cases.

Table 2 presents a similar analysis of data from Zimmer and Maynard. Size distribution data in this case were characterized by bimodal distributions representing a combination of thermally and mechanically generated particles, and the *CMD* and σ_g values characterizing the least square lognormal fit to each mode are included in the table. As in the case of the McCawley *et al.* data, errors in the estimated surface area were substantially reduced when using $\sigma_{g,est}$ = 1.8. S_R values covered the range 1.65–3.05 for $\sigma_{g,est}$ = 1.8, with the highest aerosol surface areas once again being associated with the lowest values of S_R. Table 3 gives the results of a similar analysis with $\sigma_{g,est}$ = 1.8, but with different values of $d_{n,min}$ and $d_{m,min}$. Reducing $d_{n,min}$ to 10 nm (representing the use of an instrument such as the TSI 3007 portable CPC) greatly increases the error in the estimated surface area in all cases except hardwood. Similarly, large increases in S_R are seen as the minimum detection diameter of the aerosol photometer is raised to 0.3 μm, indicating that in this case the estimated surface area may be critically dependent on the operating range of the instruments used.

DISCUSSION

As would be expected, each analysis above demonstrates that estimating aerosol surface area using two independent measurements will be prone to errors in the estimated value, and depending on the aerosol and the assumptions made, these errors may be a factor of two or more greater than the estimated quantity. Errors of this magnitude would generally be considered untenable in the process of quantifying an aerosol exposure. However, for the purpose of identi-

Table 2. S_R calculated using measured aerosol size distributions from Zimmer and Maynard (2002), assuming $\sigma_{g,est}$ = 1.3, and $\sigma_{g,est}$ = 1.8. $d_{n,min}$=0.02 μm, $d_{n,max}$ = 1 μm, $d_{m,min}$ = 0.1 μm, $d_{m,max}$ = 4 μm

Substrate	Lognormal fit to data			$\sigma_{g,est}$ = 1.3		$\sigma_{g,est}$ = 1.8	
	CMD (μm)	σ_g	*N* (no./m^3)	Estimated surface area (cm^2/m^3)	S_R	Estimated surface area (cm^2/m^3)	S_R
Hardwood	0.035	1.58	7.08×10^{11}	136.14	2.20	80.56	1.83
	2.637	2.00	2.00×10^{7}				
PTFE	0.010	1.69	6.06×10^{10}	2.38	4.31	1.69	3.07
	2.305	1.36	4.62×10^{5}				
Aluminum	0.011	7.78	1.17×10^{11}	3.16	3.41	1.75	1.90
	–	–	–				
Steel	0.010	1.80	7.54×10^{10}	3.37	2.86	2.41	2.05
	–	–	–				
Granite	0.010	1.78	1.09×10^{10}	3.58	2.98	2.72	3.03
	0.913	1.56	1.83×10^{7}				
Ceramic	0.010	1.75	3.97×10^{10}	44.43	2.12	34.07	1.66
	0.669	2.33	4.58×10^{8}				

For each substrate the lognormal parameters of each mode within the measured size distribution are given.

fying exposure trends and semi-quantitative exposure levels, the proposed analysis may be feasible.

Consideration of unimodal lognormal distributions indicates that measurement errors may be kept within 100% for count median diameters between 0.03 and 2 μm with no *a priori* knowledge of the distribution width (Figs 2 and 3). Single mode aerosols are most likely to be associated with processes involving one dominant generation mechanism, such as welding, smelting and powder handling. In these cases, calculations indicate that semi-quantitative estimates of aerosol surface area may be feasible. However, there will be many cases where multiple generation mechanisms lead to the development of multi-modal distributions. The extreme case will occur where aerosols are simultaneously present from nucleation processes and mechanical processes.

Estimating aerosol surface area for bimodal distributions assuming realistic instrument responses leads to significantly greater errors. Figure 8 indicates estimated surface area to lie between two and nine times the actual value over a range of bimodal size distributions, although for many of the distributions the difference between estimated and actual values is much less than a factor of 9. In all cases surface area is overestimated. Instrument operating ranges are highly influential in determining error, with narrower ranges reducing the error substantially (Fig. 9).

The analysis of the McCawley *et al.* data (Table 1) generally supports the estimated error from sampling a unimodal lognormal distribution, although the measured distributions are only approximated by lognormal distributions. Generally, the distributions measured by McCawley *et al.* are characterized by geometric standard deviations between 1.5 and 2. Correspondingly, assuming a standard deviation of 1.8 gave substantially better estimates of the aerosol surface area. Thus, the analyses indicate that for single mode aerosols where some information on the probable distribution width is available, the proposed method will provide reasonable estimates of surface area much of the time.

Single mode aerosols are most likely to be associated with processes involving one dominant generation mechanism, such as welding, smelting and powder handling. However, there will be many cases where multiple generation mechanisms lead to the development of multi-modal distributions. The extreme case will occur where aerosols are simultaneously present from nucleation processes and mechanical processes, as is the case with high speed grinding. The bimodal distributions reported by Zimmer and Maynard represent the extreme case where coagulation rates are low, leading to a nucleation mode below 10–20 nm. In many workplaces particle number concentrations are likely to be sufficiently high to increase the count median diameter of this mode substantially. Thus, the Zimmer and Maynard data probably represent a more extreme situation than would be encountered in many workplaces.

Estimating aerosol surface area from the Zimmer and Maynard data assuming instrument operating ranges established at the beginning of the paper lead to estimated values in the range 2.1–4.3 times the actual value assuming a geometric standard deviation of 1.3, and between 1.7 and 3.1 times the actual value assuming a geometric standard deviation of 1.8 (Table 2). As was found previously, assuming a higher value of $\sigma_{g,est}$ leads to smaller errors in the estimated surface area with real size distributions. It is important to note that for the bimodal distribution errors were always positive—surface area is overestimated in each case.

Table 3. S_R calculated using measured aerosol size distributions from Zimmer and Maynard (2002), assuming $\sigma_{g,est}$ = 1.8, $d_{n,max}$ = 1 μm and $d_{m,max}$ = 4 μm

Substrate	Lognormal fit to data			$d_{n,min}$=0.01 μm, $d_{m,min}$=0.1 μm		$d_{n,min}$=0.02 μm, $d_{m,min}$=0.3 μm	
	CMD (μm)	σ_g	*N* (no./m^3)	Estimated surface area (cm^2/m^3)	S_R	Estimated surface area (cm^2/m^3)	S_R
Hardwood	0.035	1.7	8.0×10^{11}	86.07	1.86	171.01	3.70
	3.800	1.5	1.2×10^{7}				
PTFE	0.010	1.7	8.0×10^{10}	3.37	6.12	3.05	5.53
	2.000	1.5	8.5×10^{5}				
Aluminum	0.011	1.8	1.2×10^{11}	3.36	3.64	3.75	4.05
	0.600	1.8	5.0×10^{6}				
Steel	0.010	1.7	8.0×10^{10}	4.39	3.72	3.98	3.38
	0.850	1.5	6.0×10^{6}				
Granite	0.010	1.7	1.0×10^{10}	4.20	4.68	3.13	3.48
	0.800	1.7	1.9×10^{7}				
Ceramic	0.010	1.7	5.0×10^{10}	53.11	2.59	34.78	1.70
	0.700	1.9	4.0×10^{8}				

For each substrate the lognormal parameters describing the nucleation and coarse modes in each distribution are given.

Table 4. Comparing S_R calculated using measured aerosol size distributions from Zimmer and Maynard (2002) [S_R(data)], to S_R calculated using bimodal lognormal distributions characterized by the nucleation and coarse modes for each substrate [S_R(bimodal)]

Substrate	Distribution parameters		$\sigma_{g,est}$ = 1.3		$\sigma_{g,est}$ = 1.8	
	α	β	S_R(data)	S_R(bimodal)	S_R(data)	S_R(bimodal)
Hardwood	10.4	–4.8	2.95	2.59	1.83	1.61
PTFE	14.1	–5.0	4.31	5.10	3.07	3.78
Aluminum	7.4	–4.4	3.41	3.86	1.90	1.31
Steel	9.2	–4.1	2.86	4.26	2.05	3.08
Granite	8.9	–2.7	3.98	4.03	3.03	3.06
Ceramic	8.4	–2.1	2.17	2.75	1.66	2.10

The range of errors in Table 2 qualitatively agrees well with those estimated for bimodal distributions. Table 4 compares the estimated error assuming bimodal distributions characterized by the nucleation and coarse modes in each measured distribution, to those estimated from the actual data. As can be seen, there is fair agreement. In nearly every case S_R estimated directly from the data is lower than that estimated from the bimodal distribution, confirming the bimodal case to give an upper estimate of the errors associated with the method. The theoretical analysis is therefore supported as providing a reasonable indication of the error limits associated with applying the method to bimodal aerosols.

Table 3 clearly demonstrates that the operating ranges of the instruments used to measure particle number and mass concentration are critical to the accuracy of the estimate of surface area. In general the influence of instrument operating range is in line with that seen with ideal lognormal distributions. Changes in estimated measurement error are closely dependent on the aerosol size distribution, and about the only firm conclusion that can be drawn from Table 3 is that reducing the CPC lower limit or increasing the photometer lower limit increases the estimation error in most cases. However, all estimated surface area values remain well with an order of magnitude of the actual value.

Clearly the degree to which estimated surface area is predicted to agree with actual surface area, particularly in the case of bimodal distributions, is far in excess of the errors usually associated with exposure measurements. It would therefore be unwise to propose this method of estimating aerosol surface area as a substitute for more rigorous approaches. However, at the same time it must be acknowledged that there is currently no practical method available to measure aerosol surface area *in situ*. Plotting the data from Tables 1 and 2 as estimated versus actual surface area (Fig. 10) shows that estimation errors are relatively small compared to the range of surface area values. Correlation between estimated and calculated values is good when considering both values of $\sigma_{g,est}$ used, and is very good for a single value of $\sigma_{g,est}$, indicating

that a simple calibration function could be used to improve the accuracy of surface area estimates. Thus, even with estimated values up to four times the actual value, this method should be suitable to place exposures into coarse categories (such as high/medium/low). While such measurements would not be suitable for evaluating exposure against surface area based exposure limits, they may well be sufficient to indicate whether surface area correlates more closely with health effects than mass concentration in some cases. Certainly the results of this analysis would seem sufficiently encouraging to support evaluation of the method in the field.

SUMMARY

This analysis has shown using aerosol number and mass concentration measurements should give a reasonable estimate of particulate surface area in unimodal lognormal distributions if a reasonable estimate of the geometric standard deviation is used. For bimodal distributions, estimated surface area is predicted to be as high as nine times the actual surface area in extreme cases, with the surface area being overestimated and dependent on the operating range of each instrument used. Using published workplace aerosol size distribution data, it has been shown that surface area may be estimated to better than a factor of six of the actual value in many cases from measurements of aerosol number and mass concentration. With some knowledge of the aerosol distribution, it should be possible using the analysis presented to reduce estimate errors further. Controlling the operating range of the instruments also lends itself to obtaining more accurate estimates of aerosol surface area. It must be recognized, however, that these figures have been calculated assuming a well-defined instrument response. In the case of photometers, dependence on particle density, and to a lesser extent shape and diameter, will lead to additional errors.

Although the estimated errors are high, the accuracy of surface area estimates using this method does lend itself to identifying exposure hot spots using widely available instruments. More importantly, where measurements of aerosol number and mass concentration are frequently made in parallel, the method provides a means of estimating aerosol surface area exposure with little additional work. In the absence of widespread alternative measurement methods, the use of parallel CPC and aerosol photometer measurements may offer a plausible route to preliminary investigations associating surface area to health effects in the workplace, pending the development and acceptance of more appropriate instruments.

NOMENCLATURE

CMD	=	particle count median diameter
$\overline{CMD}$	=	geometric mean *CMD* of two lognormal distributions
d	=	particle diameter
$d_{i,\min}$	=	minimum particle diameter detectable when measuring quantity *i*
$d_{i,\max}$	=	maximum particle diameter detectable when measuring quantity *i*
$\mathrm{d(norm)}_{i,\min}$	=	$d_{i,\min}$ normalized by *CMD*
$\mathrm{d(norm)}_{i,\max}$	=	$d_{i,\max}$ normalized by *CMD*
$d_{\bar{m}}$	=	diameter of average mass
$d_{\bar{s}}$	=	diameter of average surface area
M_i	=	measured value of aerosol quantity *i*
N	=	particle number concentration
C_i	=	expected value of aerosol quantity *i*
R_i	=	instrument response when measuring aerosol quantity *i*
S_{actual}	=	actual aerosol surface area
S_{est}	=	estimated aerosol surface area
S_{R}	=	relative estimated surface area
w	=	weighting factor
$\%\Delta S$	=	error in estimated aerosol surface area
$\%\Delta S_{\max}$	=	$\%\Delta S$ associated with a subset of parameters α and β
$\%\Delta S_{\max,\mathrm{norm}}$	=	normalized $\%\Delta S_{\max}$
α	=	function relating the modal *CMD*s of a bimodal distribution
β	=	function relating the modal number concentrations in a bimodal distribution
σ_i	=	standard deviation associated with measurement of quantity *i*
σ_{g}	=	geometric standard deviation
$\sigma_{\mathrm{g,est}}$	=	estimated σ_{g} of an assumed lognormal distribution
γ_i	=	total concentration of quantity *i*
$\gamma_i MD$	=	median diameter associated with quantity *i*
χ	=	minimization function
ρ	=	particle density

APPENDIX: EXAMPLE CALCULATIONS OF AEROSOL SURFACE AREA ESTIMATION FROM NUMBER AND MASS CONCENTRATION MEASUREMENTS

These iterative calculations have been written in Excel (Microsoft, USA), but can be adapted for most spreadsheet applications.

For the calculations to run correctly, iterations must be enabled in the spreadsheet. If using Excel, the Analysis Toolpak add-in needs to be installed to use the error function. If the iterative calculation does not run correctly at first, it can be forced by entering a nominal value for Est[i] CMD (B21), then re-entering the correct formula. Figure A1 shows an sample spreadsheet.

Example spreadsheet

	A	B	C	D
6	**PARAMETER**	**VALUE**	**UNITS**	**NOTES**
7	**Instrument operating limits**			
8	dnmin	2.00E-08	m	Minimum diameter for number concentration measurements
9	dnmax	1.00E-06	m	Maximum diameter for number concentration measurements
10	dmmin	5.00E-07	m	Minimum diameter for mass concentration measurements
11	dmmax	2.50E-06	m	Maximum diameter for mass concentration measurements
12	**Constants**			
13	Particle Density	2000	kg/m3	
14	CMD_first_est	5.00E-07	m	Starting estimate for distribution Count Median Diameter
15	Convergence_Test	0.1	%	Target % difference between iterative estimates of CMD
16	GSD	2		Assumed distribution Geometric Standard Deviation
17	**Measured Values**			
18	nmeas	8.40E+09	particles/m3	Measured number concentration
19	mmeas	1.78E-08	kg/m3	Measured mass concentration
20	**Iterations**			
21	Est[i] CMD	8.54E-08	m	*i* th estimate of CMD
22	Est MMD	3.61E-07	m	Estimated Mass Median Diameter
23	Ln(dnmin/CMD)/(2*Ln(GSD))	-1.047		⌈ Lower and upper integration limits
24	Ln(dnmax/CMD)/(2*Ln(GSD))	1.775		⌊ to estimate number concentration n
25	Ln(dmmin/MMD)/(2*Ln(GSD))	0.235		⌈ Lower and upper integration limits
26	Ln(dmmin/MMD)/(2*Ln(GSD))	1.396		⌊ to estimate mass concentration m
27	n	9.08E+09	particles/m3	Estimated actual number concentration
28	m	5.14E-08	kg/m3	Estimated actual mass concentration
29	n/m	1.76E+17		n/m from Equation 6
30	Est[i+1] CMD	8.54E-08	m	Revised estimate of CMD using equation 8
31	**Convergence Test**	Convergence		Check whether solution for CMD has converged
32	**Surface Area**	5.44E-04	m2/m3	Estimated aerosol surface area

Associated Formulas

	A	B	C
6	**PARAMETER**	**FORMULA**	**UNITS**
7	**Instrument operating limits**		
8	dnmin		m
9	dnmax		m
10	dmmin		m
11	dmmax		m
12	**Constants**		
13	Particle Density		kg/m3
14	CMD_first_est		m
15	Convergence_Test		%
16	GSD		
17	**Measured Values**		
18	nmeas		particles/m3
19	mmeas		kg/m3
20	**Iterations**		
21	Est[i] CMD	IF(TYPE(B30)=1,B30,B14)	m
22	Est MMD	B21*EXP(3*LN(B16)^2)	m
23	Ln(dnmin/CMD)/(2*Ln(GSD))	LN(B8/B21)/(2*LN(B16))	
24	Ln(dnmax/CMD)/(2*Ln(GSD))	LN(B9/B21)/(2*LN(B16))	
25	Ln(dmmin/MMD)/(2*Ln(GSD))	LN(B10/B22)/(2*LN(B16))	
26	Ln(dmmin/MMD)/(2*Ln(GSD))	LN(B11/B22)/(2*LN(B16))	
27	n	2*B18/(SIGN(B24)*ERF(ABS(B24))-SIGN(B23)*ERF(ABS(B23)))	particles/m3
28	m	2*B19/(SIGN(B26)*ERF(ABS(B26))-SIGN(B25)*ERF(ABS(B25)))	kg/m3
29	n/m	B27/B28	
30	Est[i+1] CMD	(1/EXP(1.5*LN(B16)^2))*((B28/B27)*6/(PI()*B13))^(1/3)	m
31	**Convergence Test**	IF(100*((B30-B21)/B21)<B15,"Convergence","No Convergence")	
32	**Surface Area**	B27*PI()*(B30*EXP(LN(B16)^2))^2	m2/m3

Fig. A1. Example spreadsheet and associated formulas.

REFERENCES

Baltensperger U, Weingartner E, Burtscher H, Keskinen J. (2001) Dynamic mass and surface area measurements. In Baron PAB, Willeke K, editors. Aerosol measurement. Principles, techniques and applications. 2nd edn. New York: Wiley-Interscience. pp. 387–418.

Brown DM, Wilson MR, MacNee W, Stone V, Donaldson K. (2001) Size-dependent proinflammatory effects of ultrafine polystyrene particles: a role for surface area and oxidative stress in the enhanced activity of ultrafines. Toxicol Appl Pharmacol; 175: 191–9.

Brunaeur S, Emmett PH, Teller E. (1938) Adsorption of gases in multimolecular layers. J Am Chem Soc; 60: 309.

Driscoll KE. (1999). Rat lung tumour responses to poorly-soluble particles: Mechanistic considerations and implications for occupational exposure guidelines. In Shuker L, Levy L, editors. IEH report on approaches to predicting toxicity from occupational exposure to dusts. Report R11. Norwich: Page Bros. pp. 17–26.

Gäggeler HW, Baltensperger U, Emmenegger M *et al.* (1989) The epiphaniometer, a new device for continuous aerosol monitoring. J Aerosol Sci; 20: 557–64.

Hatch T, Choate SP. (1929) Statistical description of the size properties of non-uniform particulate substances. J Franklin Inst; 207: 369.

Keller A, Fierz M, Siegmann K, Siegmann HC, Filippov A. (2001) Surface science with nanosized particles in a carrier gas. J Vacuum Sci Technol A Vacuum Surfaces Films; 19: 1–8.

Lison D, Lardot C, Huaux F, Zanetti G, Fubini B. (1997) Influence of particle surface area on the toxicity of insoluble manganese dioxide dusts. Arch Toxicol; 71: 725–9.

McCawley MA, Kent MS, Berakis MT. (2001) Ultrafine beryllium aerosol as a possible metric for chronic beryllium disease. Appl Occup Environ Health; 16: 631–8.

Oberdörster G. (2000) Toxicology of ultrafine particles: in vivo studies. Phil Trans R Soc London Series A; 358: 2719–40.

Oberdörster G, Gelein RM, Ferin J, Weiss B. (1995) Association of particulate air pollution and acute mortality: involvement of ultrafine particles? Inhal Toxicol; 7: 111–24.

Pandis SN, Baltensperger U, Wolfenbarger JK, Seinfeld JH. (1991) Inversion of aerosol data from the epiphaniometer. J Aerosol Sci; 22: 417–28.

Rogak SN, Flagan RC, Nguyen HV. (1993) The mobility and structure of aerosol agglomerates. Aerosol Sci Technol; 18: 25–47.

Tran CL, Buchanan D, Cullen RT, Searl A, Jones AD, Donaldson K. (2000) Inhalation of poorly soluble particles. II. Influence of particle surface area on inflammation and clearance. Inhal Toxicol; 12: 1113–26.

Woo K-S, Chen D-R, Pui DYH, Wilson WE. (2001) Use of continuous measurements of integral aerosol parameters to estimate particle surface area. Aerosol Sci Technol; 34: 57–65.

Zimmer AT, Maynard, AD. (2002) Investigation of the aerosols produced by a high-speed, hand-held grinder using various substrates. Ann Occup Hyg; 46: 663–72.